A PROCESS DIRECTION DYNAMIC MODEL FOR HIGH PRECISION WEB/BELT TRANSPORT SYSTEMS

By

Ming Yang[1]
Xerox Research Center Webster
USA

ABSTRACT

This article proposes a process direction dynamic model for closed loop belts and open loop webs used in high precision transport systems such as those found in printers where micron level registration is required. It gives the detailed derivation of the lumped parameter-based, elastically-stretchable dynamic model and shows that the angular velocities of the rolls, instead of the surface velocities of the belts/webs, should be the variables directly used in the governing equations. It discusses the effects of traction as well as disturbance sources such as roll eccentricities and the drag from stationary rolls (backer-bars). The focus of this article is on the enhanced inertia compensated tension rolls (dancers) which may be used in either open loop webs or closed loop belts (US patents pending). The design formula of the enhanced inertia compensated tension rolls takes into consideration the belt/web elasticity, belt/web tension and wrap angle. Validation of the model by other numerical methods and experiments is also discussed at the end of this article.

NOMENCLATURE

A_i	angle of wrap of web/belt at a roll
b	belt/web thickness
B_{vi}	viscous (damp) constant of a roll
D_i	drag force applied at a stationary roll
E	belt/web Young's modulus of elasticity
e_i	radial eccentricity amplitude of a roll
J_i	moment of rotational inertia of a roll

[1] The author would like to thank Barry Mandel, William Nowak, Bin Zhang, Elias Panides and his other Xerox colleagues for their many valuable suggestions and discussions and he would like to particularly thank William Nowak, Roger Leighton and Thomas Wyble for their work in the validation experiments.

K	electromotive force constant of a DC motor
K_{dm}	torsion spring stiffness of the driving shift
k_i	tensional spring constant at a tensional roll
L	electric inductance in a motor
L_i	belt/web span length between two rolls
M_i	mass of a roll
N_i	normal force on a roll
Q_i	applied torques at a roll
R	electric resistance in a motor
r_i	external radius of a roll
R_i	external radius of a roll plus half belt thickness ($R_i = r_i + b/2$)
S_i	belt/web tangential displacement at the inner surface of a roll along belt moving direction
T_i	belt/web Tension with a span
w	belt/web width
α	belt/web entrance and exit angles at a tensional roll
ω	angular velocity of a roll
θ	rotation angle of a roll
μ	frictional coefficient between belt/web and roll external surface

INTRODUCTION

Both closed loop belts and open loop webs are commonly used in high precision transport systems such as printers where micron level registration is required. In a printer, for example, closed loop belts may be used as photoreceptors to develop images which either transfer the images directly to media (paper) or transfer the image to another belt or roll. Closed loop belts may also be used as intermediate belts which are intermediate carriers for the images, and they can also serve as escort belts to transport media precisely. Open loop webs are usually the media itself which are continuously fed to one or more image stations to be imaged and transported out to receive different kinds of finishing procedures.

The motion quality of belts/webs in high precision transport systems includes components in both the process (longitudinal) direction and the cross-process (lateral) direction and this article will concentrate on the process direction while the study of the cross-process direction dynamics will be published in another paper. It should be pointed out that both process and cross-process direction dynamics in web handlings have been studied by various authors. For example, in 1993, K. Reid and K. Lin presented their study on the time domain response in process direction for a dancer subsystem when a sinusoidal disturbance is applied at one of the rolls [1]; in 1995, J. Ries published his results on the longitudinal dynamics of a winding zone [2]; and in 1997 B. Boulter showed research results on the effect of speed loop bandwidths and line speed on a system eigenvalues in multi-span web transport systems (without a dancer or tension roll) [3].

GOVERNING EQUATIONS OF BELT/WEB DYNAMICS

Let's start with one rotational roll (roll # i) in the web/belt system, and assume T_i^{en} and T_i^{ex} are the tension forces applied at the entrance and exit places of the rotational roll (Q_{Ti}^{en} and Q_{Ti}^{ex} are the applied torques by the corresponding tension forces), ω_i is the roll

angular velocity, θ_i is the rotational angle, and J_i is the moment of rotational inertia of the roll. We have

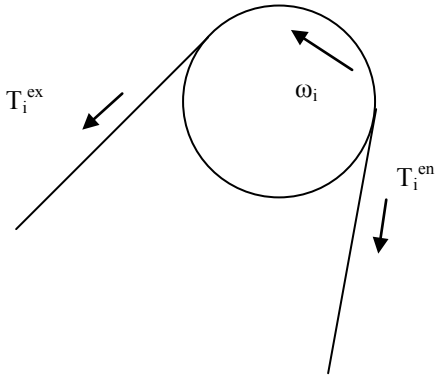

Figure 1– Belt Moving around a Roll

$$J_i \frac{d\omega_i}{dt} = J_i \frac{d^2\theta_i}{dt^2} = Q_{Ti}^{ex} - Q_{Ti}^{en} - B_{vi}\omega_i + Q_i \qquad \{1\}$$

where B_{vi} is the viscous constant representing the dampening effect of the roll assembly to the motion, Q_i is the combined toque applied by: 1)the driving motor, 2) other dragging/action mechanism, and/or 3) the eccentric force if the geometric center of the roll is off the rotational center.

To consider the stretch of the web/belt, we need to establish the relationship between the belt tension and belt displacement and roll angular velocity. To derive this relationship, we will make the assumption that the belt has no mass. This assumption should be quite a realistic one since the belt mass is usually much smaller than the roll's mass. For a mass-less belt, within a span connecting two rolls, the belt displacement follows the standard stress and strain law.

Let's assume S_i is the belt displacement at the belt center between the inner and external surfaces on roll i along belt moving direction, and L_i is the span length between the rotational roll *i* and the rotational roll *i+1*. Assume also there is one stationary roll/backing bar (so a drag force is applied there, and assuming roll ik denotes the kth stationary roll along belt span i) or one other kind of drag force located between rotational roll i and i+1 (Figure 2); assume D_{ik} is the drag force applied at this stationary roll/intermediate location; and assume L_{ik}^o and L_{ik}^i are the span lengths between the stationary roll to rotational roll i+1 and rotational roll i ($L_i = L_{ik}^i + L_{ik}^o$). We can find that the belt tension and displacement have the following relationship according to elasticity theory:

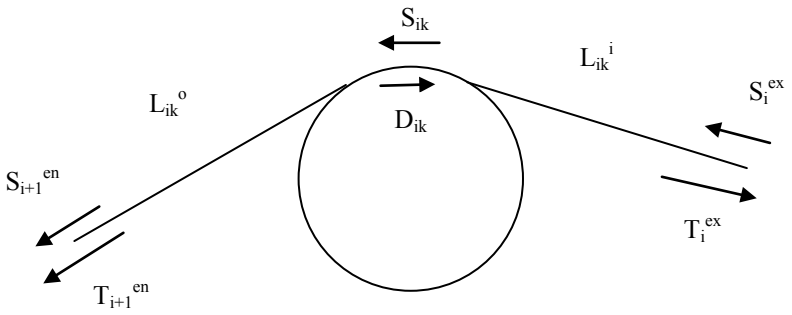

Figure 2 – Drag or Frictional Force at Stationary Roll ik

$$T_{i+1}^{en} = T_i^{ex} + D_{ik} \quad \{2\}$$

$$S_{ik} - S_i^{ex} = \frac{L_{ik}^i T_i^{ex}}{Ebw} \quad \{3\}$$

$$S_{i+1}^{en} - S_{ik} = \frac{L_{ik}^o T_{i+1}^{en}}{Ebw} \quad \{4\}$$

Summing up equation {3} and {4}, noting equation {2} and $L_i = L_{ik}^i + L_{ik}^o$, and taking a derivative with respect to time (the need to take a derivative is such that the belt speed is easily related to the angular velocity of the rotational roll, which will become apparent later.), we have:

$$\frac{dT_i^{ex}}{dt} = \frac{Ebw}{L_i}\left(\frac{dS_{i+1}^{en}}{dt} - \frac{dS_i^{ex}}{dt}\right) - \frac{L_{ik}^o}{L_i}\frac{dD_{ik}}{dt} \quad \{5\}$$

$$\frac{dT_{i+1}^{en}}{dt} = \frac{Ebw}{L_i}\left(\frac{dS_{i+1}^{en}}{dt} - \frac{dS_i^{ex}}{dt}\right) + \frac{L_{ik}^i}{L_i}\frac{dD_{ik}}{dt} \quad \{6\}$$

Note from equation {5} and {6}, the tension at the exit point of roll i is identical to the tension at the entrance point of roll i+1 if there is no stationary roll (or there is no friction on the stationary roll surface) and if there is no drag force applied between the two rotational rolls.

If the drag force is due to the friction between the stationary roll and the belt/web, assuming the normal force is N_{ik}, the frictional coefficient is μ_{fk}, and the wrap angle at the stationary roll is A_{ik}, the frictional drag force is

$$D_{ik} = N_{ik}\mu_{fk} \approx (T_i^{ex} + T_{i+1}^{en})\mu_{fk} \sin\frac{A_{ik}}{2} \quad \{7\}$$

Combining Equation {5} to {7}, and defining a frictional force influence coefficient as:

$$K_{fik} = \frac{2\mu_{fk} \sin\frac{A_{ik}}{2}}{1 - \frac{L^i_{ik} - L^o_{ik}}{L_i}\mu_{fk} \sin\frac{A_{ik}}{2}} \qquad \{8\}$$

we have:

$$\frac{dT^{ex}_i}{dt} = \frac{Ebw}{L_i}\left(\frac{dS^{en}_{i+1}}{dt} - \frac{dS^{ex}_i}{dt}\right)\left(1 - K_{fik}\frac{L^o_{ik}}{L_i}\right) \qquad \{9\}$$

$$\frac{dT^{en}_{i+1}}{dt} = \frac{Ebw}{L_i}\left(\frac{dS^{en}_{i+1}}{dt} - \frac{dS^{ex}_i}{dt}\right)\left(1 + K_{fik}\frac{L^i_{ik}}{L_i}\right) \qquad \{10\}$$

If along the span between rotational roll i and i+1, there is more than one friction force from stationary rolls and/or more than one dragging force which may not be expressed in equation {7}, equations {5}, {6}, {9} and {10} should be modified to be generalized as:

$$\frac{dT^{ex}_i}{dt} = \frac{Ebw}{L_i}\left(\frac{dS^{en}_{i+1}}{dt} - \frac{dS^{ex}_i}{dt}\right)\left(1 - \sum_{ik} K_{fik}\frac{L^o_{ik}}{L_i}\right) - \frac{dD^{ex}_{edi}}{dt} \qquad \{11\}$$

$$\frac{dT^{en}_{i+1}}{dt} = \frac{Ebw}{L_i}\left(\frac{dS^{en}_{i+1}}{dt} - \frac{dS^{ex}_i}{dt}\right)\left(1 + \sum_{ik} K_{fik}\frac{L^i_{ik}}{L_i}\right) + \frac{dD^{en}_{edi+1}}{dt} \qquad \{12\}$$

where

$$\frac{dD^{ex}_{edi}}{dt} = \sum_{ik}\frac{L^o_{ik}}{L_i}\frac{dD_{ik}}{dt}; \quad \frac{dD^{en}_{edi+1}}{dt} = \sum_{ik}\frac{L^i_{ik}}{L_i}\frac{dD_{ik}}{dt}$$

To solve equation {1}, we still need to establish a relationship between the belt speed and the roll angular velocity. This relationship, however, depends on how we treat the contact interface between the roll's external surface and the belt's inner surface. Depending on the contact conditions, we may generalize the contact interfaces into two kinds of assumptions and thus we have two sets of relations, i.e. two versions of algorithms to solve the belt dynamical problems.

A) Assume belt is inextensible on the belt/roll contact segment and belt has exactly the same speed at the inner surface as the roll's external surface all over the contact zone:

In this case, if we assume R_i is the roll external radius plus half of the belt thickness, i.e. $R_i = r_i + b/2$ if we define r_i as the roll radius (when there is eccentricity, the roll radius will be different at different locations at different times and we will use R^{en}_i, R^{bi}_i and

R_i^{ex} to denote the roll radii (plus half belt thickness) at the belt entrance, the bisector and the exit locations around the contact zone between belt and roll), the belt speed at a regular non-tensional roll is:

$$\begin{aligned} \frac{dS_i^{ex}}{dt} &= \omega_i R_i^{ex} \\ \frac{dS_i^{en}}{dt} &= \omega_i R_i^{en} \end{aligned} \qquad \{13\}$$

At a tension roll, the tension spring displacement S_t will contribute to the effective span elongation as shown in Figure 2, and the effective velocity, assuming the tension roll is roll ti, becomes:

$$\begin{aligned} \frac{dS_{t_i}^{en}}{dt} &= \omega_{ti} R_{ti}^{en} + \cos\alpha_{ti}^{en} \frac{dS_t}{dt} \\ \frac{dS_{t_i}^{ex}}{dt} &= \omega_{ti} R_{ti}^{ex} - \cos\alpha_{ti}^{ex} \frac{dS_t}{dt} \end{aligned} \qquad \{14\}$$

Note also the applied torques from the belt tensions are:

$$\begin{aligned} Q_{Ti}^{ex} &= T_i^{ex} R_i^{ex} \\ Q_{Ti}^{en} &= T_i^{en} R_i^{en} \end{aligned} \qquad \{15\}$$

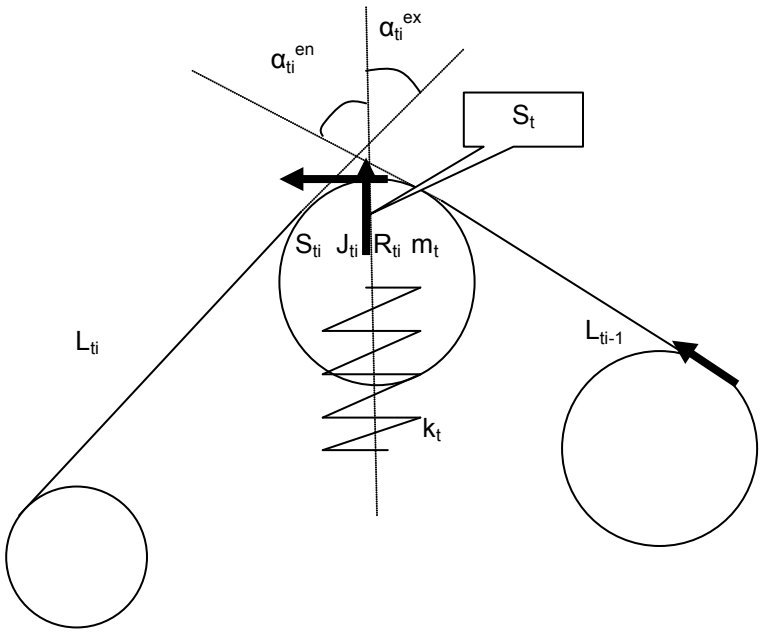

Figure 3 – Tension Spring

If we define an effective torque/force derivative due to drags as:

$$\frac{dQ_{edi}}{dt} = -\sum_{ik} \frac{dD_{ik}}{dt} \frac{L^o_{ik}}{L_i} R^{ex}_i - \sum_{(i-1)k} \frac{dD_{(i-1)k}}{dt} \frac{L^i_{(i-1)k}}{L_{i-1}} R^{en}_i \qquad \{16a\}$$
$$= -R^{ex}_i \frac{dD^{ex}_{edi}}{dt} - R^{en}_i \frac{dD^{en}_{edi-1}}{dt}$$

and the derivative of all the applied force/torque as:

$$\frac{dQ_{Ai}}{dt} = \frac{dQ_{edi}}{dt} - B_{vi} \frac{d\omega_i}{dt} + \frac{dQ_i}{dt} \qquad \{16b\}$$

Using equations {11}, {12}, {13} and {15}, we can rewrite the dynamic equation {1} for a roll which is not next to a tension roll (after taking a derivative with respect to time) into:

$$J_i \frac{d^2\omega_i}{dt^2} = Ebw\{\frac{R^{en}_{i+1}\omega_{i+1} - R^{ex}_i \omega_i}{L_i}(1 - \sum_{ik} K_{fik} \frac{L^o_{ik}}{L_i})R^{ex}_i \qquad \{17\}$$
$$-\frac{R^{en}_i \omega_i - R^{ex}_{i-1}\omega_{i-1}}{L_{i-1}}(1 + \sum_{(i-1)k} K_{f(i-1)k} \frac{L^i_{(i-1)k}}{L_{i-1}})R^{en}_i\} + \frac{dQ_{Ai}}{dt}$$

Assuming the tension roll is roll *ti*, from equations {11} and {12}, and using equations {14} and {15}, we have the dynamic equation at the tension roll as:

$$J_{ti} \frac{d^2\omega_{ti}}{dt^2} = Ebw\{\frac{R^{en}_{ti+1}\omega_{ti+1} + \cos\alpha^{ex}_{ti} \frac{dS_t}{dt} - R^{ex}_{ti}\omega_{ti}}{L_{ti}}(1 - \sum_{tik} K_{ftik} \frac{L^o_{tik}}{L_{ti}})R^{ex}_{ti} \qquad \{18\}$$
$$-\frac{R^{en}_{ti}\omega_{ti} + \cos\alpha^{en}_{ti} \frac{dS_t}{dt} - R^{ex}_{ti-1}\omega_{ti-1}}{L_{ti-1}}(1 + \sum_{(ti-1)k} K_{f(ti-1)k} \frac{L^i_{(ti-1)k}}{L_{ti-1}})R^{en}_{ti}\} + \frac{dQ_{Ai}}{dt}$$

Similarly, the dynamic equations for rolls just before and after the tension roll are:

$$J_{ti-1} \frac{d^2\omega_{ti-1}}{dt^2} = Ebw\{\frac{R^{en}_{ti}\omega_{ti} + \cos\alpha^{en}_{ti} \frac{dS_t}{dt} - R^{ex}_{ti-1}\omega_{ti-1}}{L_{ti-1}}(1 - \sum_{(ti-1)k} K_{f(ti-1)k} \frac{L^o_{(ti-1)k}}{L_{ti-1}})R^{ex}_{ti-1} \qquad \{19\}$$
$$-\frac{R^{en}_{ti-1}\omega_{ti} - R^{ex}_{ti-2}\omega_{ti-2}}{L_{ti-2}}(1 + \sum_{(ti-2)k} K_{f(ti-2)k} \frac{L^o_{(ti-2)k}}{L_{ti-2}})R^{en}_{ti-1}\} + \frac{dQ_{Ati-1}}{dt}$$

$$J_{ti+1}\frac{d^2\omega_{ti+1}}{dt^2}=Ebw\{\frac{R^{en}_{ti+2}\omega_{ti+2}-R^{ex}_{ti+1}\omega_{ti+1}}{L_{ti+1}}(1-\sum_{(ti+1)k}K_{f(ti+1)k}\frac{L^{o}_{(ti+1)k}}{L_{ti+1}})R^{ex}_{ti+1}$$
$$-\frac{R^{en}_{ti+1}\omega_{ti+1}+\cos\alpha^{ex}_{ti}\frac{dS_t}{dt}-R^{ex}_{ti}\omega_{ti}}{L_{ti}}(1+\sum_{tik}K_{fik}\frac{L^{i}_{tik}}{L_{ti}})R^{en}_{ti+1}\}+\frac{dQ_{Ati+1}}{dt} \quad \{20\}$$

Assuming the tension roll mass is M_t, the translational motion of the tensional spring is:

$$M_t\frac{d^2S_t}{dt^2}=-K_tS_t-T^{ex}_{ti}\cos\alpha^{ex}_{ti}-T^{en}_{ti}\cos\alpha^{en}_{ti} \quad \{21\}$$

Using equations {11} and {12}, and defining an effective force derivative due to drags as:

$$\frac{dD_{edt}}{dt}=\cos\alpha^{ex}_{ti}\sum_{tik}\frac{dD_{tik}}{dt}\frac{L^{o}_{tik}}{L_{ti}}-\cos\alpha^{en}_{ti}\sum_{(ti-1)k}\frac{dD_{(ti-1)k}}{dt}\frac{L^{i}_{(ti-1)k}}{L_{ti-1}}$$
$$=\cos\alpha^{ex}_{ti}\frac{dD^{ex}_{edti}}{dt}-\cos\alpha^{en}_{ti}\frac{dD^{en}_{edti-1}}{dt} \quad \{22\}$$

we have the equation governing the disturbance component of the translational motion of the spring:

$$M_t\frac{d^3S_t}{dt^3}=-K_t\frac{dS_t}{dt}-Ebw\cos\alpha^{ex}_{ti}\left(\frac{R^{en}_{ti+1}\omega_{ti+1}+\cos\alpha^{ex}_{ti}\frac{dS_t}{dt}-R^{ex}_{ti}\omega_{ti}}{L_{ti}}\right)(1-\sum_{tik}K_{dtik}\frac{L^{o}_{tik}}{L_{ti}}) \quad \{23\}$$
$$-Ebw\cos\alpha^{en}_{ti}\left[\frac{R^{en}_{ti}\omega_{ti}+\cos\alpha^{en}_{ti}\frac{dS_t}{dt}-R^{ex}_{ti-1}\omega_{ti-1}}{L_{ti-1}}\right](1+\sum_{(ti-1)k}K_{d(ti-1)k}\frac{L^{i}_{(ti-1)k}}{L_{ti-1}})+\frac{dD_{edt}}{dt}$$

B) Assume belt's inner surface has exactly the same speed as the roll's external surface at the bisector of the contact zone and all belt segments follow the stress and strain relation elsewhere:

In this case, if we assume there is eccentricity in (rotational) roll i (Figure 4), and A_i is the wrap angle, and S^r_{ei} ($V^r_{ei}=dS^r_{ei}/dt$) is the transversal displacement (velocity) (in roll radial direction along the wrap bisector line) of the belt at the bisector on roll i due to eccentricity (positive displacement is pointing away from the belt loop), the belt speeds at the belt entrance and exit places on a regular non-tensional roll are:

$$\frac{dS_i^{ex}}{dt} = \omega_i R_i^{bi} - \frac{dS_{ei}^r}{dt}\sin(0.5A_i)$$
$$\frac{dS_i^{en}}{dt} = \omega_i R_i^{bi} + \frac{dS_{ei}^r}{dt}\sin(0.5A_i) \qquad \{24\}$$

At a tension roll, as discussed before, the tension spring displacement S_t will contribute to the effective span elongation as shown in Figure 2, and the effective velocity, assuming the tension roll is roll ti, becomes:

$$\frac{dS_{t_i}^{en}}{dt} = \omega_{ti} R_{ti}^{bi} + \frac{dS_{ei}^r}{dt}\sin(0.5A_i) + \cos\alpha_{ti}^{en}\frac{dS_t}{dt}$$
$$\frac{dS_{t_i}^{ex}}{dt} = \omega_{ti} R_{ti}^{bi} - \frac{dS_{ei}^r}{dt}\sin(0.5A_i) - \cos\alpha_{ti}^{ex}\frac{dS_t}{dt} \qquad \{25\}$$

Replacing equations {13} to {14} with equations {24} and {25} in the roll and tension spring dynamic equations {17} to {23}, we shall arrive at a set of similar equations which are the dynamic equations in contact condition Case B. The equations are not listed here to save space, but a simple way to get that set of equations from equations in Case A is by replacing all radii at entrance and exit points with the radius at the bisector and adding an equivalent drag force from the effect of the radial/transversal velocity component due to the eccentricity at the end of each equation. The equivalent drag torque from the effect of the radial velocity component due to the eccentricity at all the rolls is:

$$Q_{ei}^r = EbwR_i^{bi}\{\frac{S_{ei+1}^r\sin(0.5A_{i+1}) + S_{ei}^r\sin(0.5A_i)}{L_i}(1 - \sum_{ik} K_{fik}\frac{L_{ik}^o}{L_i})$$
$$-\frac{S_{ei}^r\sin(0.5A_i) + S_{ei-1}^r\sin(0.5A_{i-1})}{L_{i-1}}(1 + \sum_{(i-1)k} K_{f(i-1)k}\frac{L_{(i-1)k}^i}{L_{i-1}})\} \qquad \{26\}$$

Cg: Geometry Center
Cr: Rotational Center
e: Eccentricity
Ψ0: Initial phase of eccentricity
Ψ: angle to interested point

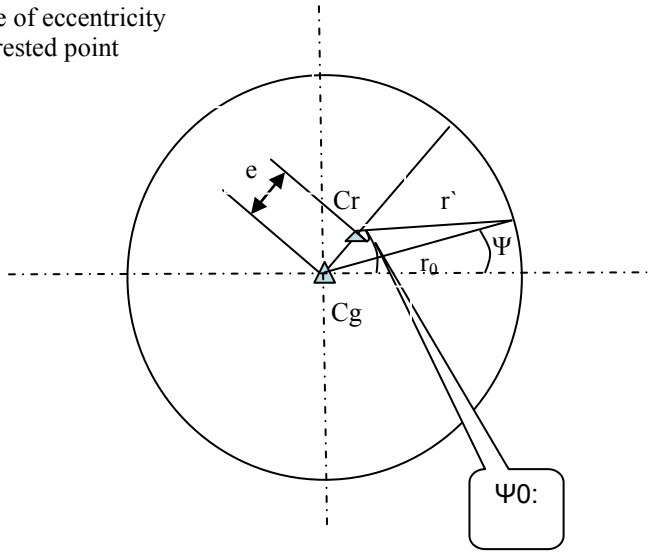

Figure 4 – Eccentricity

And for the tensional spring, the added equivalent drag force from the effect of the radial velocity component at the neighboring rolls due to the eccentricity is:

$$Q_{ei}^{r} = -Ebw\{\frac{S_{ei+1}^{r}\sin(0.5A_{i+1}) + S_{ei}^{r}\sin(0.5A_{i})}{L_i}(1-\sum_{ik}K_{fik}\frac{L_{ik}^{o}}{L_i})\cos\alpha_{ti}^{ex} + \frac{S_{ei}^{r}\sin(0.5A_{i}) + S_{ei}^{r}\sin(0.5A_{i-1})}{L_{i-1}}(1+\sum_{(i-1)k}K_{f(i-1)k}\frac{L_{(i-1)k}^{i}}{L_{i-1}})\cos\alpha_{ti}^{en}\} \quad \{27\}$$

ECCENTRICITY CONDITION

When there is eccentricity on a roll like what is shown on Figure. 4, the effective radius r_i (which is location and time dependent) is related to the geometric radius r_{0i} by:

$$r_i^2 = r_{0i}^2 + e_i^2 - 2e_i r_{0i}\cos(\underline{\Omega}_i t + \psi_{0i} - \psi_i) \quad \{28\}$$

Or since the eccentricity e_i is much smaller than the radius r_i and r_{oi}, we have:

$$r_i \approx r_{0i} - e_i\cos(\underline{\Omega}_i t + \psi_{0i} - \psi_i) \quad \{29\}$$

$$S_{ei}^{r} \approx r_i - r_{0i} = -e_i\cos(\underline{\Omega}_i t + \psi_{0i} - \psi_i) \quad \{30\}$$

Equation {29} shall be used in finding out the instantaneous radii at the entrance, at the bisector and at the exit of each of all the rolls when eccentricities are presented, and similarly, equation {30} shall be used in finding out the equivalent drag force in equation {26} and {27} when the contact condition Case B is adapted.

ACTION FORCES/TORQUES

The derivatives of all the effective action torque applied at each of the rolls can be separated into three components:

$$\frac{dQ_i}{dt} = \frac{dQ_{mi}}{dt} + \frac{dQ_{ai}}{dt} + \frac{dQ_{ei}}{dt} \qquad \{31\}$$

where the first component Q_{mi} is supplied by the motor so that it is non-zero only at the driver roll. If we assume K_{dm} is the torsion spring of the driving shaft, θ_{md} and θ_d are the rotational angles at the shaft's two ends: one attached to the motor and the other to the driver roll (note if we assume θ_m is the motor, G_{md} is the gear ratio of the motor to driver roll angular velocities, θ_{md} can be expressed as $\frac{d\theta_{md}}{dt} = \frac{1}{G_{md}}\frac{d\theta_m}{dt} = \frac{r_m}{r_{md}}\frac{d\theta_m}{dt}$), we have: $Q_{mi} = K_{dm}(\theta_{md} - \theta_d)$. The second component Q_{ai} is due to drag because of some dragging action mechanism including impact from any disturbance sources. The last component Q_{ei} is due to torque generated by the gravity force when rolls have eccentricity. Assuming the roll mass is M, the eccentricity component is

$$Q_{ei} = M_i g e_i \cos(\underline{\Omega}_i t + \psi_{0i}) \qquad \{32\}$$

Note equation {31} does not include the equivalent drag force/torque given by equations {26} and {27} which are equivalent drags from the radial/transversal velocity due to the eccentricity. This item exists only in contact condition Case B where the belt and roll surface are assumed to have the same speed at the contact bisector (same process velocity at the bisector).

DRIVER CONDITION

Assuming θ_m is the rotational angle of the motor, the motion of a DC motor can be described by the following equation:

$$J\frac{d^2\theta_m}{dt^2} + b_m\frac{d\theta_m}{dt} + K_{dm}(\theta_{md} - \theta_d) = Ki \qquad \{33\}$$

where J is the moment of inertia of the motor assembly (equivalent inertia up to the driver shift), b_m is the mechanical damping coefficient for the motor, K is the electromotive force constant, and i is the armature current of the motor.

Four different motor driver conditions have been considered in this analysis:

1) The motor keeps constant angular velocity;
2) The motor keeps constant torque, i.e. the armature current of the motor is kept constant;

3) The motor is controlled by a servo and its armature current/voltage is a function of the speed or displacement measured at an encoder: a) If the current is directly controlled by the servo, equation {33} may be used directly to analyze the motor motion; b) if the voltage is specified instead, the following equation is required to find the relationship between the current and the voltage.

$$L\frac{di}{dt} + Ri = V - K\frac{d\theta}{dt} \qquad \{34\}$$

where L is the electric inductance, R is the electric resistance, and V is the voltage of the driving motor.

4) The motor is a stepper and its motion is controlled by the servo which used the speed or displacement measured at an encoder as its input.

BOUNDARY CONDITIONS IN OPEN LOOP WEBS

An open loop web differs from a closed loop belt in that there are two end rolls in a web and there the belt is not constrained by the previous/next rolls. We can simply simulate the web by a closed loop belt if we assume the next/previous roll for one end roll is the other end roll located an infinite distance away.

NUMERICAL SOLUTION METHODS

The set of dynamic equations in this analysis are second (or third) order differential equations. When there is no frictional force (we assume no frictional force in calculating system eigen-values and eigenvectors, i.e. assume the influence to the system eigen-values and eigenvectors due to the frictional force is small), the stiffness matrix is symmetric and the mass matrix is diagonal and therefore, the general Jacobi transformation method [4] may be used to find the eigen-values (resonance frequencies) and eigenvectors. To solve for the time responses, the fifth order Runge-Kutta method with an adaptive step size control algorithm [5] has been used and no extra assumptions about the magnitudes of the frictional and other drag forces have been introduced. In this numerical method (the fifth order Runge-Kutta method with an adaptive step size control algorithm), the step size is reduced until the solution converges according to the specified tolerance and the first try of the next step size is chosen by the error size of the previous step.

INERTIA COMPENSATED ROLL

U.S. Patent 3,659,767 to J. R. Martin discloses a "dancer" roll used in web transportation [6]. The dancer roll is a roller over which the web/belt passes as it is being transported from a roll (medium source side) to another roll and a dancer roll is supported by a linear spring and may move translationally in addition to rotationally and a dancer roll is used to regulate belt tension so a dancer roll may also be referred to as a tensional roll. The dancer roll attenuates and insulates motion disturbances from reaching the motion crucial areas of the web; and if designed according to T.R. Martin's formula, the dancer roll is supposed to perform the best. The dancer roll was originally meant to be used in the open loop web transportation (the open loop web system may be simply referred to as a web), but its area of application may be expanded to include closed loop belts (simply referred to as belts in this article) as explained later in this paper.

Assuming no web stretch and no resistance from the bearing, and further assuming the web wrap angle of the dancer roll is 180 degrees, Martin [6] found that no tension disturbance can be transported from one side to the other side of a dancer roll if the dancer roll is designed according to the following formula:

$$M = \frac{J}{r^2} \qquad \{35\}$$

where M is the dancer roll mass, J is the moment of inertia and r is the external radius of the dancer roll. While this formula gives good guidance for dancer roll design, it is based on simplifications which significantly reduce its effectiveness. Specifically, the assumption that the wrap angle is 180^{o} makes it virtually impossible to be used in a closed loop belt. Based on the governing equation given above in this article (either the contact condition Case A or Case B, a more general design formula for the dancer roll can be given as the following [7, 8]:

$$M = \frac{J}{r^2}\left(1 - \frac{\underline{T}}{Ebw}\right)\sin^2(A/2) \qquad \{36\}$$

where $\underline{T}$ is the belt/web nominal tension, E is the belt/web Young's modulus, b is the belt/web thickness, w is the web/belt width and A is the wrap angle of the dancer roll.

To validate the effectiveness of the dancer roll designed according to equation {36}, we may use a four roll closed loop belt system shown in Figure 5 as an example. In this belt system, roll 1 is driven by a "perfect" roll and roll 3 is a dancer roll, and to simulate various disturbances, we will apply a sinusoidal drag force of unit amplitude with different frequencies at roll 2 and check if these disturbances will pass through the dancer roll to reach roll 4 (since the driver is assumed to be "perfect", no disturbance can be passed there. The only place the disturbances may be passed through is at the dancer roll). The results of the analysis are shown in Figure 5.

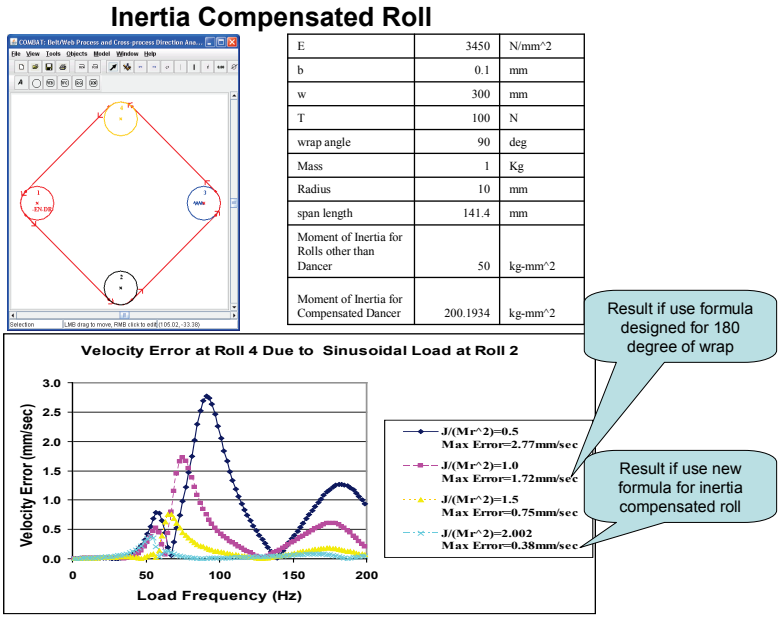

Figure 5 – Four Roll Closed Loop Belt System Using the Inertia Compensated Dancer Roll

The results in Figure 5 are obtained by changing the value of the moment of inertia of the dancer roll (roll 3) while keeping everything else constant. The peaks in the modeling results in Figure 5 actually correspond to the system resonance frequencies (which varies slightly as we change the moment of inertia of the dancer roll). From the results in Figure 5, we can see the motion error at roll 4 due to a unit amplitude sinusoidal force applied at roll 2 varies greatly as the moment of inertia of the dancer roll changes. When the ratio of $\frac{J}{Mr^2}$ changes from 0.5 (a regular solid roll) to approaching 2.002 [inertia compensated roll governed by equation {36}], the velocity error is greatly reduced from 2.77mm/sec to 0.38mm/sec. This shows how a carefully designed dancer roll may attenuate and insulate motion disturbances from reaching the motion crucial areas of a web/belt system.

MODEL VALIDATION

Extensive validation works have been performed on this web/belt dynamic model and its numerical solution methods. First, a simple two rotational roll belt system was studied using a commercial FEA package (by Bin Zhang of Xerox Corp.) and the time domain solution when an eccentricity was inputted on the driver was found to be bounded by the two results given by the two contact conditions Case A and Case B of this model. The model and the results are shown in Figure 6.

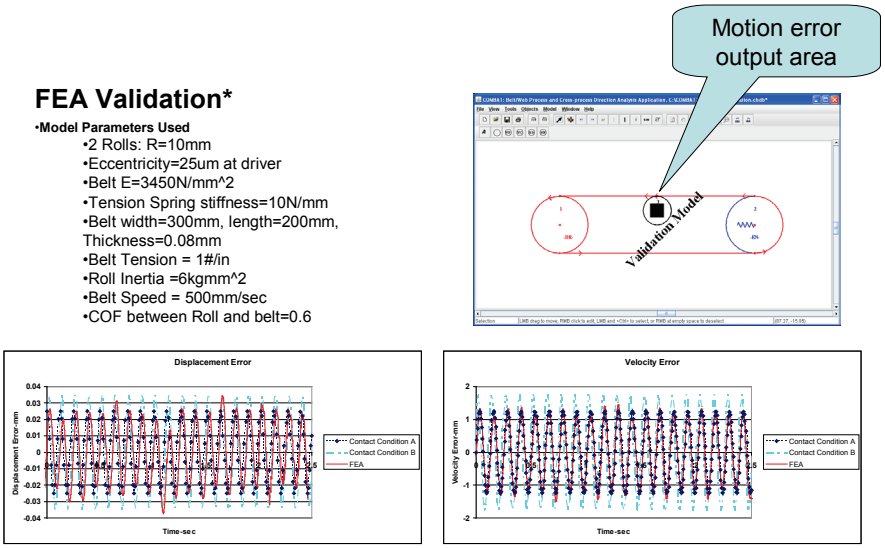

Velocity and image registration errors from FEA model are bounded by the ranges given by analysis Using Contact Condition Case A and B

*FEA model results are from Bin Zhang

Figure 6 – Two Roll belt model FEA Validation

An experiment was conducted (by Bill Nowak and Tom Wyble of Xerox Corp.) on a multiple roll closed loop belt module to validate the system resonance analysis. The comparison between the model prediction and experiments for a transfer function defined as the belt's velocity error at a particular roll's surface due to unit belt's velocity error at the driver) is shown in Figure 7 and it showed good correlation.

Resonance Frequency Validation*

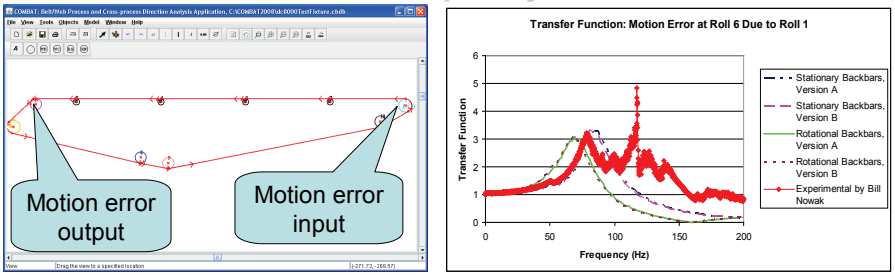

- **Models predicted the belt system had a resonance frequency at 71-85Hz (the range was due to modeling the top 4 back rolls as either rotational or stationary rolls), and experiment confirmed the resonance frequency at 78.25Hz.**
- **Experiment suggested there was another resonance frequency at around 120Hz the model did not predict. This resonance frequency seemed to come from the structure supporting the belt (Frame vibration was noticeable). This model did not consider the structural vibration.**
- **The default damping ratio of 0.1 used in the model seemed to work quite well. However, changing the damping ratio to 0.13 did make the modeling and the experiment results a little bit more closely correlated.**

*Experimental results are from Bill Nowak

Figure 7 – Validation of Resonance Frequency Analysis

SUMMARY

Two versions of belt/web dynamical models in the process direction based on the contact conditions between the belt/web and the roll external surface have been proposed in this paper. Case A (Sticking Model) assumes there is no slippage between the belt and roll interfaces along the entire contact ranges and Case B (Slipping Model) assumes the belt and the roll surface have the same speed at the bisector points of the contact zones over the belt roll interfaces (slippage may occur at all points other than the bisectors). While the sticking model should more closely match systems where the roll/belt interface has full strong traction and the slipping model should simulate a system where the roll/belt maintains only a minimum traction to ensure safe motion transaction, these two versions seems to give the actual operative range for all true belt/web systems when process direction dynamics is considered. An enhanced inertia compensated dancer/tension roll working equally well for either open loop webs or closed loop belts has been proposed based on the model given in this paper and numerical analyses such as FEA and experiments conducted at Xerox laboratory seem to have validated the modeling work of this article.

REFERENCES

1. Reid, K.N. and Lin, Ku-Chin, "Dynamic Behavior of Dancer Subsystems in Web Transport Systems," Proceedings of the Second International Conference on Web Handling, June 6-9, 1993, pp. 135-146.
2. Ries, J. P., "Longitudinal Dynamics of a Winding Zone," Proceedings of the Third International Conference on Web Handling, 1995, pp. 264-279.

3. Boulter, B. T., "The Effect of Speed Loop Bandwidths and Line Speed on a System Eigenvalues in Multi-span Web Transport Systems," Proceedings of the Fourth International Conference on Web Handling, 1997, pp. 287-305.
4. Cook, R., Malkus, D., and Plesha, M., Concepts and Applications of Finite Element Analysis, 3rd Edition, John Wiley & Sons, New York, 1989.
5. Press, W., Teukolsky, S., Vetterling, W., and Flannery, B., Numerical Recipes in C: The Art of Scientific Computing, 2nd Edition, Cambridge University Press, 1992.
6. Martin, J. R., Tension Regulation Apparatus, US Patent 3659767, May, 1972
7. Yang, M., Inertia Compensating Dancer Roll for Web Feed, US patent pending, Filed with USPTO May 2007.
8. Yang, M., Inertia Compensated Tension Roll in Closed Loop Belt Systems, US patent pending, Filed with USPTO April 2008.

A Process Direction Dynamic Model for High Precision Web-Belt Transport Systems	**M. Yang**, Xerox Corporation, USA

Name & Affiliation	**Question**
	Why did you choose 10 microns as the limit in your work?
Name & Affiliation	**Answer**
M. Yang, Xerox Corporation	Yes, 10 microns is what was selected as our goal in the project. It was quite difficult to achieve.